*American Mineralogist*
Vol. 57, pp. 1643–1663 (1972)

# VARIATION OF Si–O DISTANCES IN OLIVINES, SODAMELILITE AND SODIUM METASILICATE AS PREDICTED BY SEMI-EMPIRICAL MOLECULAR ORBITAL CALCULATIONS

S. JOHN LOUISNATHAN AND G. V. GIBBS, *Department of Geological Sciences, Virginia Polytechnic Institute and State University, Blacksburg, Virginia 24061*

ABSTRACT

Mulliken bond overlap populations, $n$(Si–O), are calculated in the extended Hückel molecular orbital (EHMO) approximation for the silicate ions in eleven olivines using the observed O–Si–O angles but with all Si–O = 1.63Å. The calculated overlap populations decrease in the order $n$[Si–O(1)] > $n$[Si–O(3)] > $n$[Si–O(2)] and are consistent with the observed variation in individual bond lengths where Si–O(1) < Si–O(3) < Si–O(2). The $n$(Si–O) calculated using the observed dimensions of the silicate ions show a well-developed correlation with the observed Si–O distances. Because of the simplifying assumptions involved in calculating Pauling's sum of electrostatic bond strengths to oxygen, all the oxygen atoms in the olivine structure have $\zeta$(O) = 2.0. However, our calculations suggest that the charges on the oxygen atoms O(1), O(2), and O(3) are not all equal. The apical oxygen O(1) is "electrostatically underbonded" relative to the basal oxygen atoms O(2) and O(3).

Si–O bond overlap populations calculated for artificially 'isolated' tetrahedra (thus removing the effect of Si–O–Si angle on $n$(Si–O)) from the structures of sodamelilite and sodium metasilicate, predict bond length variation in the right direction, suggesting that at least part of the bond length changes in a silicate ion can be rationalized in terms of non-equivalent hybridization characteristics of the Si atom resulting from O–Si–O angular distortions.

## INTRODUCTION

In a previous paper (Louisnathan and Gibbs, 1972b), we found that semi-empirical molecular orbital calculations based on extended Hückel theory (EHMO) appear to give a meaningful though qualitative description of the electronic structure of orthosilicic acid, $H_4SiO_4$, in that they bear a reasonably close similarity with results obtained by *ab initio* methods (Collins, Cruickshank, and Breeze, 1972). Moreover, we found that when O–Si–O valence angle distortions are present, the EHMO results predict a stabilization of the distorted ($SiO_4$) configuration by strengthening one or more Si–O bonds relative to others. The specific results and prediction of the calculations for hypothetically distorted $SiO_4$ tetrahedra (with all Si–O = 1.63Å) may be summarized as follows:

1. When the distortion of a silicate ion corresponds to local

$C_{3v}$ point symmetry, the calculated bond overlap populations, $n$(Si–O), for the basal bonds differ from that of the apical bond parallel to $C_3$. If the O(apical)–Si–O (basal) angles ($\alpha$) are wider than the O(basal)–Si–O(basal) angles ($\beta$), then $n$[Si–O (apical)] calculates larger than the $n$[Si–O(basal)], whereas if $\beta$ is larger than $\alpha$, then the basal bonds show larger populations.

2. Similar results were obtained for silicate ions of local $C_v$ point-symmetry. When the O–Si–O angles associated with the apical bond are the widest, and those associated with basal bond in the mirror plane are the narrowest (see Si–O(2) bond in Figure 1g of Louisnathan and Gibbs, 1972b), the overlap populations decrease in the order $n$[Si–O(apical bond[1] in mirror)] > $n$[Si–O(basal bonds not in mirror)] > $n$[Si–O(basal bond in mirror)].

3. If the distortion of O–Si–O angles corresponds to a local $C_{2v}$ point-symmetry, the two Si–O bonds that enclose the widest angles are predicted to have larger overlap populations than those that are involved with narrower angles.

4. In general, the largest overlap populations are predicted for the Si–O bonds that are involved in the widest O–Si–O angles, suggesting such bonds should be the shortest ones in the silicate ion. Conversely, the smallest overlap populations are predicted for the bonds involved in the narrowest O–Si–O angles.

5. Our calculations indicate that there need not be a *single* relationship between bond length and bond overlap population, even within a series of distorted tetrahedra all having the same local symmetry. For example, for a series of orthosilicic acid molecules with $C_{3v}$ point symmetry, the $n$[Si–O(apical)] and $n$[Si–O(basal)] show two different trends when plotted as a function of O–Si–O angle.

6. The predictions regarding bond length variations in distorted tetrahedra are identical whether or not the five Si(3$d$) valence orbitals are included in the computations.

Although these results are suggestive, they lack a quantitative basis because the various quantities (like $n$(Si–O), the net atomic charges $Q$(Si), etc.) obtained in the EHMO approximation are not absolute. The main purpose of this paper will be to compare the EHMO predictions against experimental observations, thereby placing the results

[1] For the sake of convenience the Si–O bond involving the three widest O–Si–O angles, like the Si–O(1) bond in olivines, will be called the apical bond.

of the calculations on a semi-quantitative basis for purposes of ordering and classifying Si–O bond length variation.

## EHMO Calculations for the Silicate Ions in Olivines

The observed Si–O bond lengths for the silicate ions in the olivines studied by Birle, Gibbs, Moore, and Smith (1968) and Brown and Gibbs (in prep.) show three distinct distances[2]: apical $\langle$Si–O(1)$\rangle$ = 1.617[0.001] and basal $\langle$Si–O(2)$\rangle$ = 1.658[0.005], and $\langle$Si–O(3,3′)$\rangle$ = 1.635[0.001]Å. A negative correlation between the mean $\langle$Si–O(2,3,3′)$\rangle$ and *M*–Si distances has been interpreted as due to electrostatic repulsions between the Si and *M* cations across a shared edge (Ribbe and Gibbs, 1971; Brown and Gibbs, in prep.). Apart from this interpretation of the variation of the *mean* Si–O distances, no other mechanisms have been advanced to explain the variation of the *individual* Si–O distances. For example, there is no correlation between Si–O bond length and the electronegativity of *M*-site cations (Brown and Gibbs, in prep.) nor between the bond lengths and $\Delta\zeta$(O) (Baur, 1971) because all the oxygen atoms in the structure are charge-balanced.

The silicate ion in the olivines exhibits $C_v$ point-symmetry; the O–Si–O angles associated with the apical Si–O(1) bond are the widest, and two of those associated with the basal Si–O(2) are the narrowest (Fig. 1). The EHMO calculations for such a distorted silicate ion predict that the Si–O(1) bond should be the shortest, Si–O(2) the longest, and Si–O(3) intermediate (Louisnathan and Gibbs, 1972b). The $n$(Si–O)s calculated[3] using the O–Si–O angles as observed in forsterite and with (1) all Si–O = 1.63Å, and (2) the observed Si–O distances are plotted (Fig. 1) against the observed Si–O distances of forsterite. The overlap populations decrease in the order $n$[Si–O(1)] > $n$[Si–O(3)] > $n$[Si–O(2)] *even when all Si–O distances are assumed to be 1.63Å in the calculation,* suggesting that the variation in the O–Si–O angles may account, in part, for the observed variation of the Si–O distances.

[2] Distances given here are the mean Si–O(1), Si–O(2), and Si–O(3) bond lengths observed in first eight structures of Table 1, where the calculated e.s.d.'s are less than 0.005Å for individual bonds. Numbers in brackets are the estimated standard deviations of the mean distances.

[3] In all the calculations observed interatomic distances and bond angles (hortonolite structure, Brown and Gibbs, in prep.) were used. Valence orbital ionization potentials used in generating the $H_{ii}$ and $H_{ij}$ terms were taken from the work of Basche, Viste, and Gray (1965), Slater exponents from Clementi and Raimondi (1963). The Si(3*d*) orbitals were included for which we have used $H_{3d3d}$ = −5.5eV and $\zeta_{3d}$ = 1.0 after Gibbs *et al.* (1972).

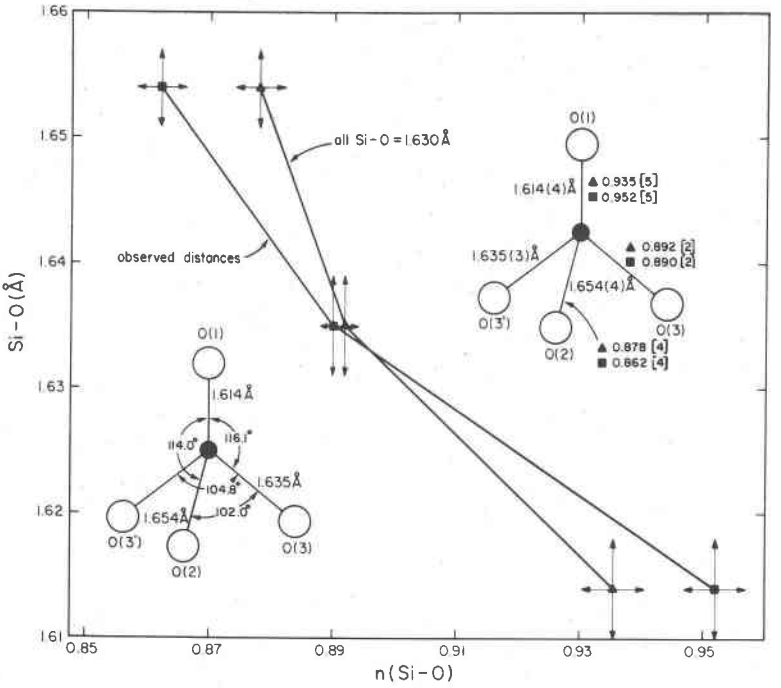


FIG. 1. Bond overlap populations for the $(SiO_4)^{4-}$ tetrahedron of forsterite. Inset tetrahedron at left shows the observed dimensions, and the one at the right shows overlap populations with maximum range of $n$(Si–O), in square brackets, for the e.s.d.s. in the bond length.

The nature of the chemical bond in an isolated silicate ion is not the same as when the ion occurs in a complex crystal structure like olivine. In order to learn how the EHMO predictions for the Si–O bond are affected by including the nearest neighbor Mg atoms and their ligands in the olivine structure, calculations for the following closed-shell complexes were undertaken:

I. $(Mg_9SiO_4)^{14+}$ group with Mg atoms in the nine nearest neighbor $M$–sites that surround the silicate ion. Only the 3$s$ valence orbitals of Mg were included in the calculation.

II. $[Mg_9(SiO_4)F_{31}]^{17-}$ complex where the F atoms were chosen to represent (1) the octahedral ligands of the Mg atoms, and (2) the second and third anion–neighbors of Si. Only the 3$s$ orbitals on Mg and 2$p$ on F were included in the calculation (the VOIP of F(2$s$) are considerably larger than those of F(2$p$) and accordingly may be considered as not appreciably involved

in $\sigma$–bonding (Gray, 1964). Fluorine rather than oxygen atoms were chosen because with F atoms the residual charge on the complex is smaller, more closely approximating a neutral complex. Moreover, with the existing capabilities of our version of the EHMO program, substantial computational time is saved by using only three valence orbitals on F (three $2p$) rather than four ($2s$ plus three $2p$) on each of the thirty–one second or third neighbor oxygen atoms of central Si atom.

III. $[Mg_9(SiO_4)F_{25}]^{11-}$ complex where the most distant six F atoms from Si were omitted and where the computation was made with the $3s$ and $3p$ orbitals on Mg.

In calculation (I), the Si···Mg interactions turned out to be weakly bonding, *i.e.*, $n$(Si–Mg) $> 0$, but on including the ligands of the Mg cations (II and III) the Si···Mg interactions became antibonding and repulsive, such repulsions being strongest when a Mg($sp$) basis set is used (III). With only $3s$ orbitals on Mg, calculation (II), Si···F (*i.e.*, silicon vs. its second or third anion neighbors) interactions are repulsive, while Mg–F (second coordination sphere) are weakly bonding. But on including the $3p$ orbitals on Mg, calculation III, all cation–anion interactions other than those of first coordination sphere are repulsive. In all the three calculations (I, II, and III), the *trends,* in $n$(Si–O) for the silicate ion remain unaltered: the apical $n$[Si–O(1)] is the largest, $n$ [Si–O(2)] the smallest and $n$[Si–O(3)] is intermediate (Fig. 2). This is in part due to the complete neglect of long range forces in the EHMO calculation and in part to the significant covalent character of the Si–O bond (Collins, *et al.*, 1972; Louisnathan and Gibbs, 1972b; Gibbs *et al.*, 1972). Results of the above calculations suggest that if we are interested in a theoretical reason for the observed *trends* in the variation of the Si–O bond length, then it may be legitimate as a first approximation to compute the overlap populations for isolated or for polymerized silicate ions, neglecting all neighboring atoms at least for structures where $\Delta\zeta(O) \sim 0$. When EHMO calculations are performed for a series of these ions then the results may be placed on a semi–quantitative basis by correlating such results with observed quantities like bond length, bond angle, *etc.* This necessitates the use of observed distortions, both in bond lengths and bond angles, in the computation. However, when observed bond lengths are used, it is difficult to assess whether the computed variation in $n$(Si–O) is due to the O–Si–O angles or to the calculated overlap integrals, $S_{ij}$, which are usually proportional to the internuclear separation, $r_{ij}$, used in the calculation. In order to avoid this complication, two sets of

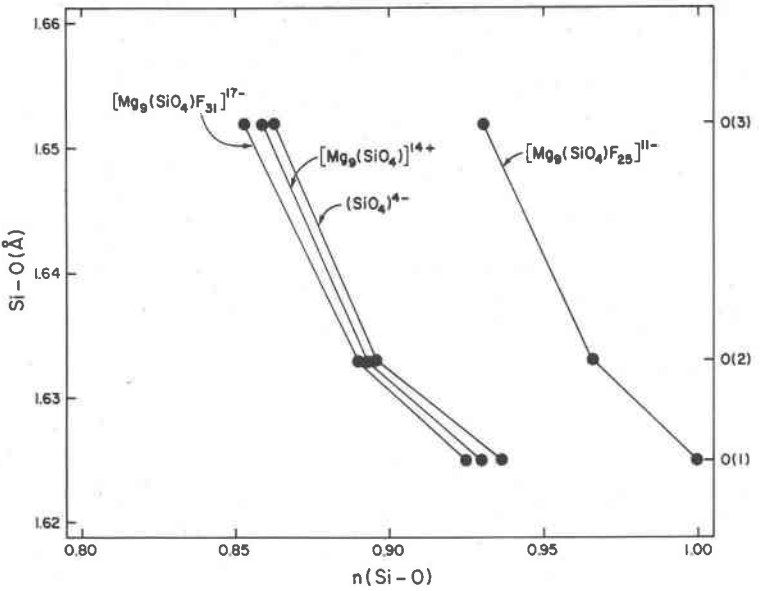


FIG. 2. Comparison of $n$(Si–O) obtained for the isolated $(SiO_4)^{4-}$ group with those obtained by introducing the $M$-cation neighbors and their ligands (see text for details).

calculations were performed using (1) a constant Si–O distance of 1.63Å and (2) the observed distances, both with observed tetrahedral valence angles (see Table 1) for eleven olivine type structures (Brown and Gibbs, in prep.). For every case a pair of calculations, one with the valence Si(*sp*) basis set and another with Si(*spd*) basis set, was undertaken.

The overlap populations computed assuming all Si–O = 1.63Å show (Fig. 3) three separate and nearly constant values for the first eight olivine structures of Table 1: 0.516(1), 0.478(5), and 0.489(1) in the Si(*sp*) basis set calculations and 0.935(2), 0.876(7), and 0.896(1) in the Si(*spd*) basis set for the Si–O(1), Si–O(2), and Si–O(3) bonds, respectively.[4] The approximate constancy in $n$[Si–O(1)], $n$[Si–O(2)], or $n$[Si–O(3)] values apparently reflects the similarity of angular geometry (Table 1) of the silicate ions in the eight olivines. In kirschsteinite and glaucochroite the O(2)–Si–O(3) angles are relatively larger (by $\sim$ 3 to 4°) than in the first eight structures, thus imparting an approximate $C_{3v}$ symmetry to their silicate ions whereby $n$[Si–O(2)] and $n$[Si–O(3)] become approximately equal. With $n$[Si–O(2)] of

[4] Mean values, with e.s.d. about the mean in parentheses are given.

TABLE 1. Si-O distances (Å), O-Si-O angles (°), bond overlap populations, and net atomic charges (e) for the $(SiO_4)^{4-}$ ions of eleven olivines.*

| | | Ni | Fo | Co | Ho | Fa | Zn-Pi | Kn | Mo | Ki | Gl | γ -Ca |
|---|---|---|---|---|---|---|---|---|---|---|---|---|
| Si-O(1) | | 1.613 (3) | 1.614 (4) | 1.613 (3) | 1.625 (4) | 1.623 (2) | 1.610 (3) | 1.619 (2) | 1.614 (4) | 1.628 (8) | 1.620 (4) | 1.637 (8) |
| Si-O(2) | | 1.663 (2) | 1.654 (3) | 1.659 (3) | 1.652 (4) | 1.655 (2) | 1.663 (4) | 1.665 (2) | 1.656 (3) | 1.643 (5) | 1.630 (5) | 1.664 (8) |
| Si-O(3) [2x] | | 1.641 (2) | 1.635 (3) | 1.637 (2) | 1.633 (3) | 1.637 (1) | 1.632 (2) | 1.629 (2) | 1.639 (2) | 1.623 (4) | 1.645 (3) | 1.642 (5) |
| O(1)-Si-O(2) | | 114.1 (2) | 114.0 (2) | 113.5 (2) | 112.8 (2) | 112.4 (1) | 113.5 (2) | 112.6 (1) | 115.8 (2) | 114.2 (3) | 114.5 (2) | 109.8 (5) |
| O(1)-Si-O(3) [2x] | | 116.4 (1) | 116.1 (1) | 116.0 (1) | 115.7 (1) | 115.7 (1) | 115.8 (1) | 115.4 (1) | 114.5 (1) | 113.6 (2) | 114.1 (1) | 115.8 (3) |
| O(2)-Si-O(3) [2x] | | 101.3 (1) | 102.0 (1) | 102.5 (1) | 102.4 (1) | 103.0 (1) | 102.3 (1) | 103.2 (1) | 102.4 (1) | 104.8 (3) | 103.7 (2) | 104.2 (3) |
| O(3)-Si-O(3') | | 105.2 (2) | 104.8 (2) | 104.7 (2) | 106.2 (2) | 105.7 (1) | 105.6 (2) | 105.7 (1) | 105.8 (1) | 104.8 (3) | 105.2 (2) | 105.7 (4) |
| n[Si-O(1)] | Si(spd) | 0.955 | 0.952 | 0.951 | 0.936 | 0.938 | 0.953 | 0.942 | 0.950 | 0.928 | 0.940 | 0.922 |
| | Si(sp) | 0.528 | 0.526 | 0.526 | 0.517 | 0.518 | 0.527 | 0.520 | 0.525 | 0.511 | 0.519 | 0.508 |
| n[Si-O(2)] | Si(spd) | 0.815 | 0.862 | 0.858 | 0.863 | 0.864 | 0.853 | 0.853 | 0.864 | 0.882 | 0.894 | 0.857 |
| | Si(sp) | 0.464 | 0.470 | 0.468 | 0.471 | 0.471 | 0.465 | 0.463 | 0.472 | 0.482 | 0.490 | 0.468 |
| n[Si-O(3)] | Si(spd) | 0.885 | 0.890 | 0.890 | 0.896 | 0.892 | 0.894 | 0.900 | 0.888 | 0.903 | 0.881 | 0.892 |
| | Si(sp) | 0.485 | 0.487 | 0.488 | 0.491 | 0.489 | 0.490 | 0.494 | 0.486 | 0.494 | 0.482 | 0.490 |
| Q(Si) | Si(spd) | +1.357 | +1.348 | +1.350 | +1.349 | +1.351 | +1.347 | +1.346 | +1.350 | +1.335 | +1.345 | +1.364 |
| | Si(sp) | +2.537 | +2.534 | +2.535 | +2.534 | +2.535 | +2.533 | +2.533 | +2.534 | +2.529 | +2.533 | +2.539 |
| $Q(O_1)$ | Si(spd) | -1.281 | -1.284 | -1.285 | -1.297 | -1.296 | -1.284 | -1.294 | -1.287 | -1.306 | -1.295 | -1.308 |
| | Si(sp) | -1.601 | -1.603 | -1.604 | -1.610 | -1.609 | -1.604 | -1.609 | -1.605 | -1.616 | -1.610 | -1.616 |
| $Q(O_2)$ | Si(spd) | -1.378 | -1.370 | -1.373 | -1.369 | -1.368 | -1.377 | -1.376 | -1.367 | -1.352 | -1.346 | -1.372 |
| | Si(sp) | -1.656 | -1.652 | -1.654 | -1.652 | -1.651 | -1.656 | -1.655 | -1.650 | -1.642 | -1.638 | -1.653 |
| $Q(O_3)$ | Si(spd) | -1.349 | -1.347 | -1.346 | -1.341 | -1.343 | -1.343 | -1.338 | -1.348 | -1.338 | -1.352 | -1.341 |
| | Si(sp) | -1.640 | -1.639 | -1.638 | -1.636 | -1.637 | -1.637 | -1.634 | -1.640 | -1.635 | -1.642 | -1.635 |

*Bond length, bond angle, and their e.s.d.s given in parentheses are from the work of Brown and Gibbs (1972) and we have used their symbols for the individual minerals. The n(Si-O), Q(Si), and Q(O) values given are for those in which observed bond lengths and bond angles were used in the EHMO calculations.

these two structures plotting close to $n$[Si–O(3)] of these and other structures, an apparent single trend between $n$[Si–O(2,3)] and Si–O bond length is developed (Fig. 3). Returning to our discussion on the first eight olivine structures, we should note that in spite of a remarkable similarity of angular distortions in the $SiO_4$ tetrahedra, individual Si–O distances do show a small range of variation in length (0.009–0.14Å). The Si–O(1) distances range between 1.610 and 1.625Å, Si–O(2) between 1.654 and 1.663Å and Si–O(3) between 1.629 and 1.641Å. Such variations are not reflected in the EHMO overlap populations (Fig. 3). Elsewhere we have suggested that the relation

$$-\Delta n/n_e = \Delta r(\text{Si–O})/r_e(\text{Si–O}) \qquad (1)$$

can be used to give a very crude estimate of bond length changes in distorted tetrahedra (Louisnathan and Gibbs, 1972a and b). Assuming an equilibrium distance, $r_e$(Si–O) = 1.63Å, and an equilibrium $n_e$(Si–O) = 0.906 [for a silicate ion of $T_d$ symmetry, with Si(*spd*) basis set, Louisnathan and Gibbs, (1972b)] equation (1) predicts nearly constant distances of Si–O(1) $\simeq$ 1.58, Si–O(2) $\simeq$ 1.68, and Si–O(3) $\simeq$ 1.65Å for all the eight structures. Setting aside the approximations involved in equation (1), the inability of the EHMO overlap populations

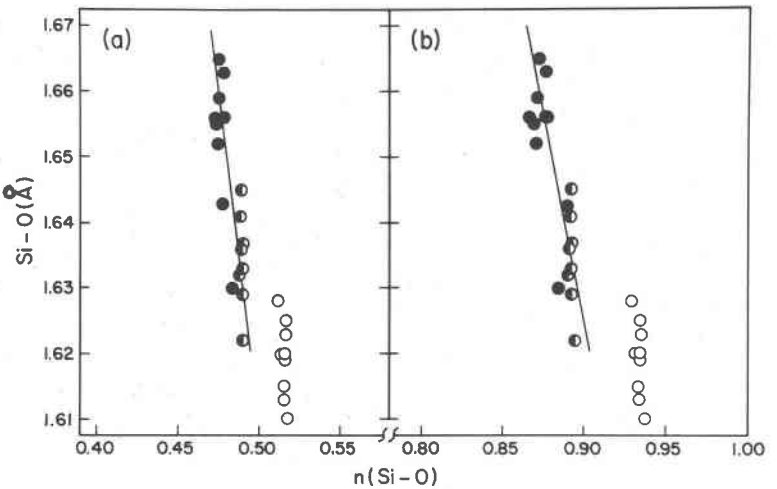


FIG. 3. Si–O bond overlap populations, $n$(Si–O), for eleven olivines (assuming all Si–O = 1.63Å, and observed angles) plotted as a function of observed Si–O distances: calculated in the (a) Si(*sp*), and the (b) Si(*spd*) basis sets. Open circles depict Si–O(1, apical), half-filled circles, Si–O(3), and filled circles, Si–O(2) bonds.

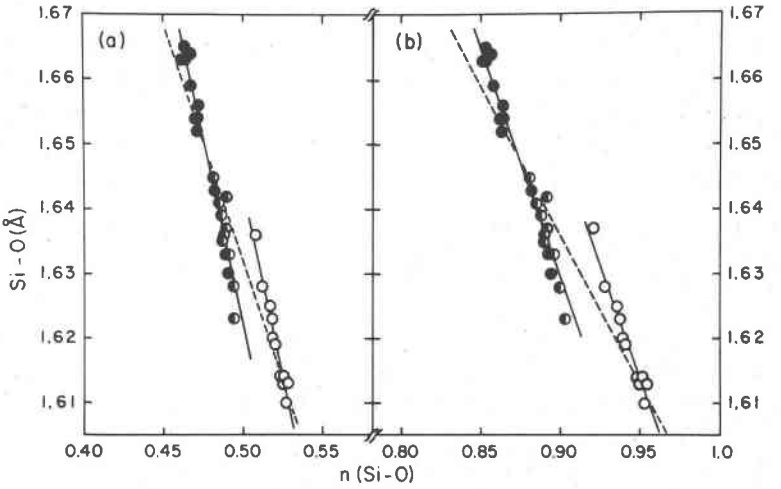


FIG. 4. Si–O bond overlap populations, $n$(Si–O), for eleven olivines, with observed dimensions, plotted against observed distances: calculated for the (a) Si(*sp*) and (b) Si(*spd*) basis sets. Symbols as in Fig. 3.

to predict small variations within each bond type [Si–O(1), Si–O(2), or Si–O(3)], may be attributed in part to (1) the total neglect of $M\cdots$Si, $M$–O, and other types of nuclear repulsive and electrostatic interactions, and (2) not simulating the non-equivalent hybridization characteristics of the oxygen atoms by omitting their nearest non-tetrahedral neighbors. The first argument is supported by the empirical evidence that the mean Si–O(2,3,3′) distances increase as the distortions in the *crystal* bring Si and $M$ ions closer together (Ribbe and Gibbs, 1971; Brown and Gibbs, in prep.) and as the $M$–O bonds decrease in length.

When the observed Si–O bond lengths are used in the calculations, two separate and well developed[5] trends emerge, (Fig. 4), one for the apical bonds, Si–O(1), and the other for the basal bonds, Si–O(2,3). The bond length–bond overlap population relationships are:

$$\text{Si}(spd)\text{ basis set: Si–O(1)} = 2.273 - 0.694n \quad (2)$$

$$\text{Si–O(2, 3)} = 2.263 - 0.704n \quad (3)$$

$$\text{Si}(sp)\text{ basis set: Si–O(1)} = 2.210 - 1.153n \quad (4)$$

$$\text{Si–O(2, 3)} = 2.195 - 1.146n \quad (5)$$

[5] The correlation coefficients are all greater than 0.93 and the student $|t|$ are all larger than 7.5.

The inherent differences in the molecular orbital characteristics about the apical and basal bonds is a cause for the two separate trends seen in Figure 4 (Louisnathan and Gibbs, 1972b). However, no quantitative significance can be attached to the separation because of the assumption that the exchange integrals, $H_{ij}$, are equal for all the basal as well as the apical bonds.

## The Variation of the Si–O Electrostatic Bond Strength in Olivines

In a previous paper (Louisnathan and Gibbs, 1972b), we have noted that Pauling's $\zeta(\mathrm{O})$ (the sum of electrostatic bond strengths reaching an oxygen) appears to simulate the electrostatic attractive energy, $U(\mathrm{O})$,

$$\zeta(\mathrm{O}) = \sum_i \frac{z_i}{\nu_i} \sim U(\mathrm{O}) = \sum_i \frac{q_i q_j}{r_{ij}}. \tag{6}$$

Because $\zeta(\mathrm{O})$ is calculated by using the nominal valences ($z_i$) and coordination number ($\nu_i$) rather than the actual charges ($q_i$) and internuclear separation ($r_{ij}$), $\zeta(\mathrm{O})$ lacks an uniform energy scale for comparing the electrostatic bond strengths of different bonds (1) in structures like olivine where neither $z_M$ nor $\nu_M$ show any variation, or (2) in going from one structure type to another. We have suggested (Louisnathan and Gibbs, 1972b) that Mulliken's (1955) *ionic bond order*

$$p_{\mathrm{ionic}}(\mathrm{Si–O}) = -Q(\mathrm{Si})Q(\mathrm{O})[0.529(\text{Å})/r(\mathrm{Si–O})(\text{Å})] \tag{7}$$

may be a better measure of the electrostatic bond strength, especially in such structures as olivine where all the oxygen atoms are charge–balanced in Pauling's model.

The net charges $Q(\mathrm{Si})$ or $Q(\mathrm{O})$, calculated in the EHMO approximation, are not absolute. However, within a given series of compounds the EHMO charges may be expected to show a correlation with the Si–O bond length. Moreover, the charges on Si or O calculated for isolated silicate ions using the observed dimensions cannot be the same as when the ions occur in a complex structure. However, our calculations (I, II, III described earlier) indicate that the *trends* in the relative charges and ionic bond orders remain unchanged (Table 2) when the next–nearest neighbors and their ligands are included. The ionic bond order of the apical Si–O(1) bond is calculated to be smaller than those of basal bonds suggesting a relative electrostatic "underbonded" character or a stronger covalent character [larger $n(\mathrm{Si–O})$] for the apical bond. The EHMO charges on apical oxygens are con-

Table 2. EHMO charges and ionic bond orders in forsterite.

| | $(SiO_4)^{4-}$ | I. $(Mg_9SiO_4)^{14+}$ | II. $[Mg_9(SiO_4)F_{31}]^{17-}$ | III. $[Mg_9(SiO_4)F_{25}]^{11-}$ |
|---|---|---|---|---|
| Q(Si) | +1.349e | +1.354e | +1.362e | +1.171e |
| Q(0,1) | -1.297 | -1.140 | -1.173 | -1.159 |
| Q(0,2) | -1.370 | -1.243 | -1.269 | -1.245 |
| Q(0,3) | -1.341 | -1.223 | -1.245 | -1.221 |
| $P_{ionic}$(Si-0,1) | 0.569a.u. | 0.502a.u. | 0.520a.u. | 0.442a.u. |
| $P_{ionic}$(Si-0,2) | 0.592 | 0.539 | 0.553 | 0.467 |
| $P_{ionic}$(Si-0,3) | 0.586 | 0.537 | 0.550 | 0.463 |

sistently lower than those for the basal oxygen atoms for all the eleven olivines, and a plot of Si–O as a function of $Q$(O) shows two separate trends, one for the apical oxygens and the other for the basal ones (Fig. 5).

Smith (1953) was the first to suggest that the bonds to underbonded ($\zeta$(O) < 2.0) oxygens are more covalent and stronger than those to overbonded oxygens. Baur (1970, 1971) has since shown that a well-developed correlation exists between $\zeta$(O) and Si–O bond length in structures where all oxygen atoms are not charge balanced. When $\zeta$(O) is plotted as a function of $n$(Si–O), Figure 6, a well-developed correlation ($r = -0.94$) results, which is consistent with Smith's (1953) original suggestion. Obviously no correlation can be made between $\zeta$(O) and $n$(Si–O) in structures where $\zeta$(O) = 2.0 for all oxygen atoms, or for those structures where the bridging oxygens (Si–O–Si) are two-coordinated.

## The Effect of O–Si–O Angular Distortions On the Si–O Bond Length

The EHMO calculations for the $(SiO_4)^{4-}$ tetrahedra in the olivine structures have borne out the predictions of our earlier calculations on hypothetically distorted tetrahedra that longer Si–O bonds should be associated with narrower O–Si–O angles and shorter ones with wider angles. When the $n$(Si–O) obtained for a series of orthosilicic acid molecules with $C_{3v}$ symmetry (Louisnathan and Gibbs, 1972b) are plotted as a function of $\langle$O–Si–O$\rangle_3$ (*i.e.*, mean of three O–Si–O angles involving a common Si–O bond) two nonlinear trends emerge (Fig. 7), both of which indicate that $n$(Si–O) of the common bond should increase with increasing $\langle$O–Si–O$\rangle_3$. Figure 8, a plot of observed Si–O distances (from a number of silicates containing isolated tetrahedra, $Si_2O_7$ ions, rings, single or double chains, and frameworks)

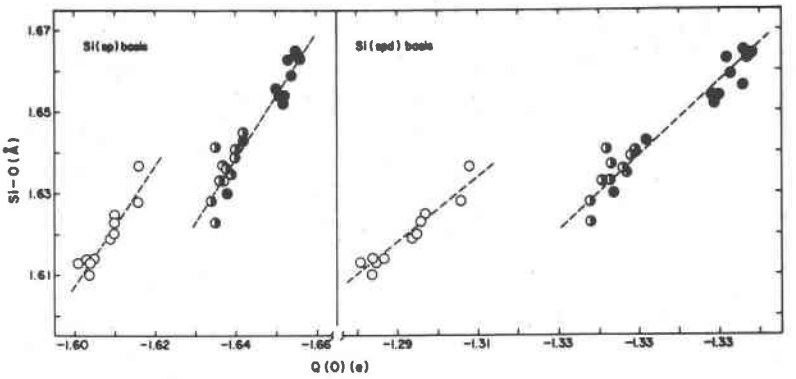


FIG. 5. EHMO charges on oxygen atoms, calculated using the observed dimensions of the $SiO_4$ group, are plotted as a function of observed Si–O distances. Symbols as in Fig. 3.

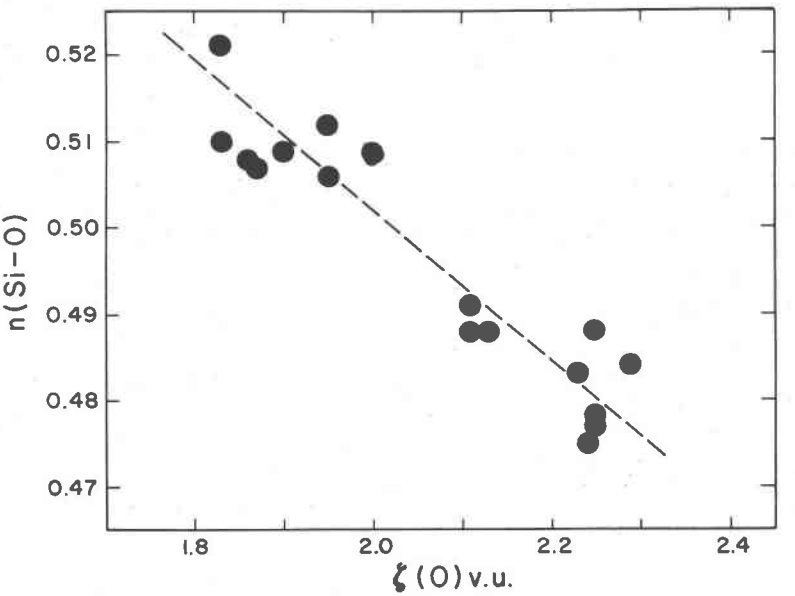


FIG. 6. $\zeta$(O) vs. $n$(Si–O) for tetrahedral bond lengths in tourmaline and margarosanite. $n$(Si–O) values, calculated with the Si($sp$) basis set with Si–O clamped at 1.63Å, are from Gibbs *et al.* (1972).

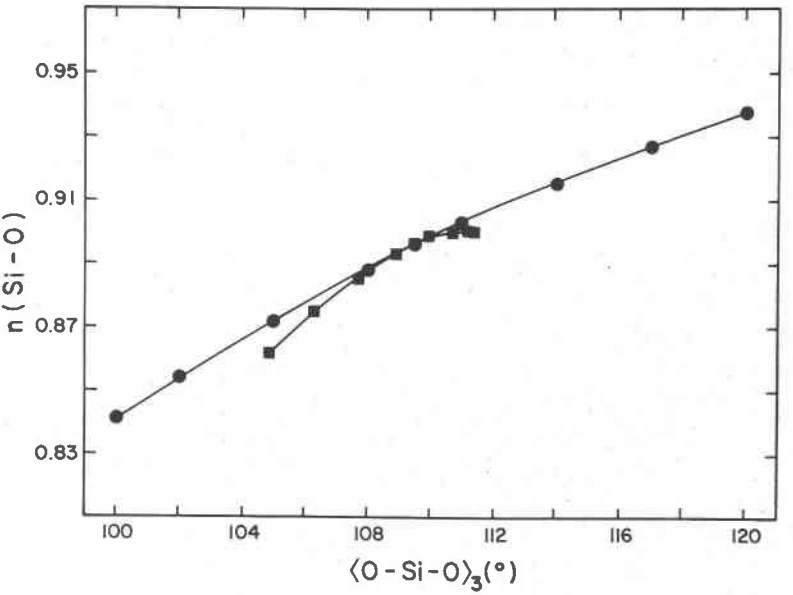


FIG. 7. Variation of $n$[Si–O (apical, circles)] and $n$[Si–O (basal, squares)] as a function of $\langle$O–Si–O$\rangle_3$ for the $H_4SiO_4$ molecule ($C_{3v}$ symmetry, all Si–O = 1.63Å, and with Si(*spd*) basis set).

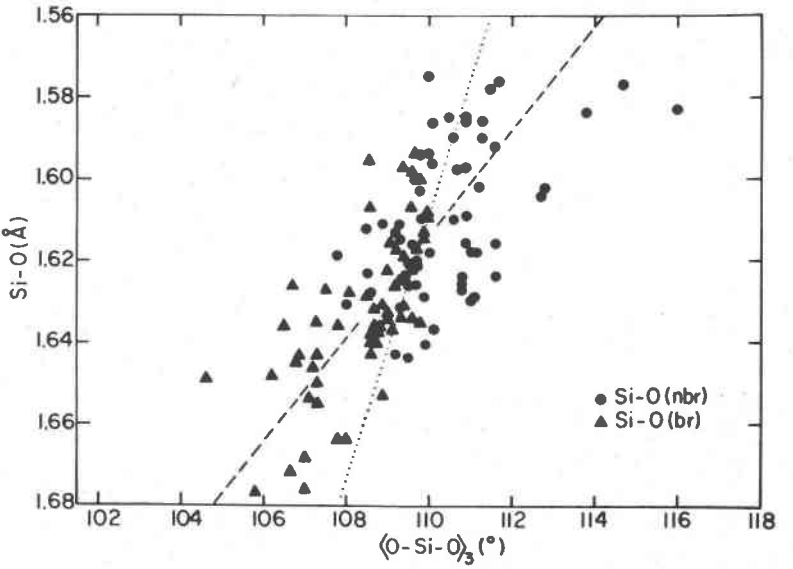


FIG. 8. The observed variation of Si–O distance with $\langle$O–Si–O$\rangle_3$ angle.

as a function $\langle O\text{–}Si\text{–}O\rangle_3$, corroborates and generalizes the aforementioned relationship between Si–O bond lengths and O–Si–O angles. McDonald and Cruickshank (1967) and Brown and Gibbs (1970) have also found that shorter Si–O distances tend to be involved in wider O–Si–O angles. The relatively large scattering of data points in Figure 8 reflects the widely varying environments of the Si–O bonds, and the existence of different nonlinear relationships for different bond types.

Baur (1970) has argued that the observed variations between Si–O distance and O–Si–O angle are a simple geometrical consequence of the movement of the silicon atom in a coordination polyhedron where all the oxygen–oxygen distances remain invariant and at constant separation. If this were approximately true, we would expect in a plot of $\langle Si\text{–}O\rangle$ vs. O···O that the data for silicates would be disturbed about a line normal to the O···O axis (see Fig. 4, McDonald and Cruickshank, 1967; Fig. 7, Brown and Gibbs, 1970). But the data actually fall about a line more nearly parallel to the O···O axis, demonstrating quite clearly that the oxygens in $SiO_4$ tetrahedra are not at constant separation as concluded by Baur but range between ~2.5 and ~2.8Å. Assuming a rigid polyhedron of four tetrahedrally disposed oxygen atoms ($T_d$ symmetry for the configuration of oxygens, with O···O distances fixed at 2.662Å) and allowing the silicon atom to move along one of the three Si–O bond directions (*i.e.*, when Si atom is considered, the silicate group would have $C_{3v}$ point symmetry unless all Si–O = 1.63Å) the geometrical relationship between Si–O bond length and $\langle O\text{–}Si\text{–}O\rangle_3$ angle is given by

$$Si\text{–}O = 4.9422 - 0.0303[\langle O\text{–}Si\text{–}O\rangle_3], \tag{8}$$

which trend is shown as a dotted line in Figure 8. This trend is significantly different from a least squares trend obtained for the observed data,

$$Si\text{–}O = 2.5589 - 0.0086(8)[\langle O\text{–}Si\text{–}O\rangle_3], \tag{9}$$

which is shown as a dashed line in Figure 8. This result suggests that although part of the relationship between Si–O bond length and O–Si–O angles can be rationalized in terms of geometrical effects, a purely geometrical model of a small hard sphere (Si-atom) rattling within a tetrahedral cavity of four larger hard spheres (O-atoms) at constant separation is inadequate to model the bond length–bond angle relationships within the $SiO_4$ tetrahedra. We assert, backed by numerous experimental observations, that O···O distances do vary as a result of polyhedra sharing their elements (Pauling, 1929 and 1960).

Such variations of O···O distances combined with other crystallochemical factors cause distortions in the tetrahedral angles (Louisnathan and Gibbs, 1972b), and the energy and shape of the *MO* wavefunctions respond to such angular distortions in establishing different $n$(Si–O) for the individual bonds in the resulting silicate ion.

The observed tetrahedral angular distortions in a series of five melilites (Smith, 1953; Louisnathan, 1969b and 1970) are similar to those observed in the olivines (Brown and Gibbs, in prep.). In melilites the variation of $\zeta$(O) is quite pronounced (*e.g.*, $\zeta(O_1) = 2.75$, $\zeta(O_2) = 1.75$, and $\zeta(O_3) = 2.00$ in hardystonite). On the other hand in olivines there is no variation in $\zeta$(O) because all oxygens are charge balanced. Yet the observed variation of individual Si–O bond lengths in melilite is quite similar to that observed in olivines. The common factor in these two series of structures is the remarkably similarity in O–Si–O angular distortions and not the variation in $\zeta$(O). This led one of us to attempt to rationalize the variation of individual bond lengths in melilites using a qualitative *MO* theory that takes into account tetrahedral angular distortions (Louisnathan, 1969b). If the variation in $\zeta$(O) is assumed to be the only factor in bond length variations, and if the tetrahedral angular distortions are a mere geometrical consequence of the Si–O distances that have varied due to $\zeta$(O), as proposed by Baur (1970, 1971), then (1) for the olivine series neither the variation in Si–O bond lengths nor the variation in O–Si–O angles can be accounted for, and (2) the predicted (using the geometrical model) O–Si–O angular distortions in melilites are gross underestimations of observed distortions as shown below for the case of hardystonite (Louisnathan, 1969a):

| angle | using the dotted line in Figure 7 (equation 8) | using Baur's (1971) equation from his table IV | observed value |
|---|---|---|---|
| $\langle O_1\text{–Si–}O_i\rangle_3$ | 108.7° | | 104.6° |
| $\langle O_2\text{–Si–}O_i\rangle_3$ | 110.9 | | 116.0 |
| $\langle O_3\text{–Si–}O_i\rangle_3$ | 109.7 | | 107.8 |
| $O_1\text{–Si–}O_2$ | | 109.5° | 111.0 |
| $O_1\text{–Si–}O_3$ | | 107.4 | 101.4 |
| $O_3\text{–Si–}O_{3'}$ | | 109.1 | 103.5 |
| $O_3\text{–Si–}O_2$ | | 111.3 | 118.5 |

In order to further assess the importance of the O–Si–O angles within a polymerized ion of $SiO_4$ tetrahedra, EHMO calculations were undertaken for the $(Si_2O_7)^{6-}$ ions in sodamelilite (Louisnathan, 1970) and for the $(SiO_3)_\infty$ metasilicate chain in $Na_2SiO_3$ (McDonald and Cruickshank, 1967). The calculation for the pyrosilicate ion consisted

of two sets of computations, one for an 'hypothetically isolated' $(SiO_4)^{4-}$ ion and another for the $(Si_2O_7)^{6-}$ group, with observed dimensions, and with Si(*spd*) as well as Si(*sp*) basis sets. Similarly two sets of computations were made for the metasilicate chain; in one the $(SiO_4)^{4-}$ tetrahedron was again treated as "isolated" but in the other four tetrahedra, $(Si_4O_{13})^{10-}$, were considered polymerized as part of a single chain like the one in $Na_2SiO_3$.

In sodamelilite, the $Si_2O_7$ group exhibits $C_{2v}$ symmetry ($C_2$ axis contains the bridging oxygen O(1), and nearly parallels the apical bond Si–O(2) where the symmetry of the individual $(SiO_4)^{4-}$ groups are $C_v$, as in olivines. Using the O–Si–O angles given in Figure 9 one can qualitatively predict the bridging Si–O(1) to be the longest and the apical Si–O(2) to be the shortest bond in the pyrosilicate ion. To obtain a semi-quantitative estimate of bond length variations, one may use the calculated $n$(Si–O) for the '*isolated*' $(SiO_4)^{4-}$ group (Fig. 9b) and using equations (2) and (3). The predicted bond lengths, Si–O(1)

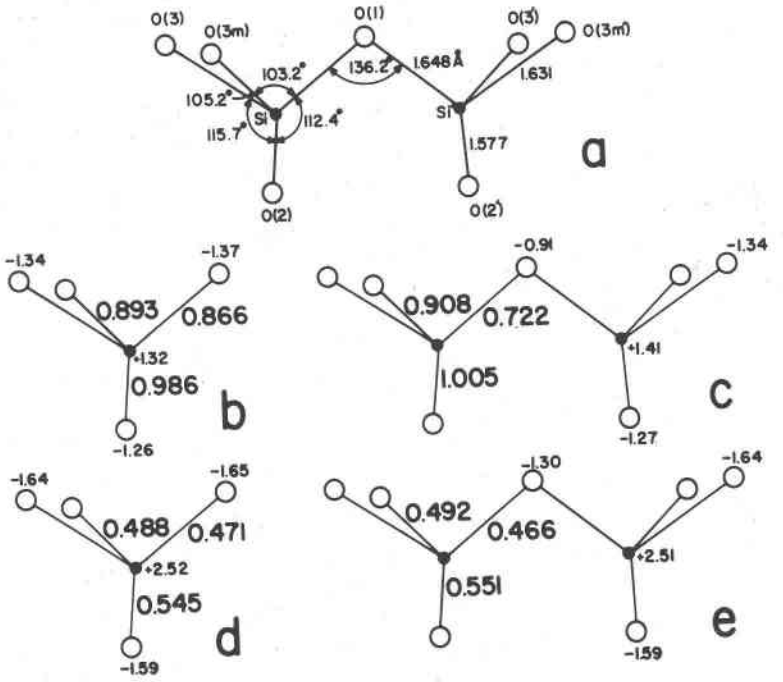


FIG. 9. Results of EHMO calculations for the $(Si_2O_7)^{6-}$ ion in sodamelilite. (a) Dimension of the pyrosilicate ion. (b) $n$(Si–O) and $Q(r)$ for the "hypothetically isolated" $(SiO_4)^{4-}$ group, and (c) for the actual $(Si_2O_7)^{6-}$ group with Si(*spd*) basis set. (d) and (e) are similar results for Si(*sp*) basis set calculations.

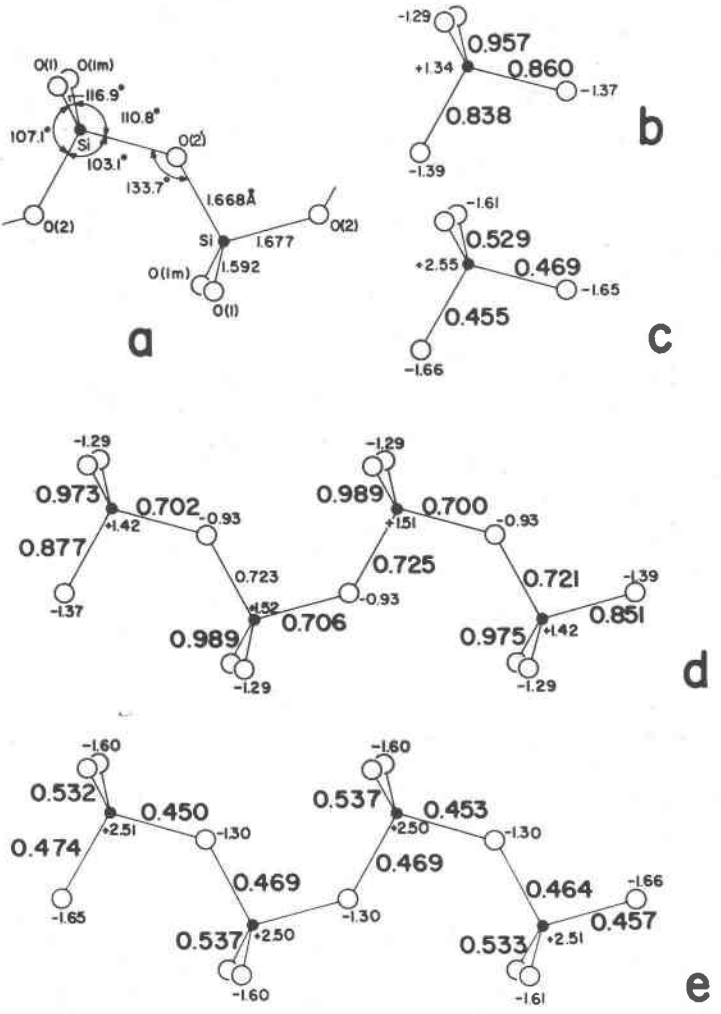


FIG. 10. Results of EHMO calculations for the $(SiO_3)_\infty$ single chain in $Na_2SiO_3$. (a) Dimensions of the chain. (b) $n$(Si–O) and $Q(r)$ for the hypothetically isolated $(SiO_4)^{4-}$ group calculated with Si(*spd*) and (c) Si(*sp*) basis sets. (d) and (e) are similar calculations for a four-membered single chain.

= 1.65, Si–O(2) = 1.59, and Si–O(3) = 1.63Å, suggest that (the nature of tetrahedral angular distortions being similar to those in olivines, *i.e.*, $C_v$ point symmetry) Si–O(1) and Si–O(2) will plot on the line of basal bonds and the apical Si–O(2) with the apical bonds of olivines (Fig. 4). In $Na_2SiO_3$ metasilicate, the local symmetry of the $(SiO_4)^{4-}$ group is nearly $C_{2v}$ (Fig. 10). The O(1)–Si–O(1*m*) is the

largest tetrahedral angle (116.9°); therefore, it is expected Si–O(1) be shorter than Si–O(2) as observed (Louisnathan and Gibbs, 1972b). With an Si–O–Si angle of 133.7°, the general relationship between Si–O(br) and Si–O–Si angle suggests a significantly shorter (~1.635Å) Si–O(2;br) bond than the observed lengths of 1.677–1.668Å (McDonald and Cruickshank, 1967; Brown and Gibbs, 1970; Gibbs *et al.*, 1972). Our calculations suggest that the 'extra' lengthening of Si–O(2) may be explained in part in terms of the narrow O–Si–O angles associated with it. The observation that EHMO results for 'hypothetically isolated' $(SiO_4)^{4-}$ groups with observed distortions as in a polymerized tetrahedral ion, can reasonably predict the observed variations in Si–O bond length, suggests that the O–Si–O angles within a tetrahedron may play a more important role than forces from outside the tetrahedron. When polymerized ions, rather than hypothetically separated ions are considered, the role played by Si–O–Si valence angles is properly taken into account in the EHMO calculations, a problem that has been investigated at length by Gibbs *et al.* (1972). In the crystal structure of zunyite (Louisnathan and Gibbs, 1972a), the Si–O–Si bonds are all linear within the $(Si_5O_{16})^{12-}$ ion, which according to a more commonly observed trend between Si–O–Si and Si–O(br) would indicate Si–O(br) bonds to be shorter than the Si–O(nbr) bonds. However, all the Si–O bonds are statistically identical, 1.63Å, and all the O–Si–O angles close to the ideal angle of 109.5°. Fairly extensive EHMO calculations for the $(Si_2O_7)^{6-}$ ion ($D_{3h}$ symmetry) predicts that the Si–O(br) will be shorter than the Si–O(nbr) only when the O(br)–Si–O(nbr) angles are wider than O(nbr)–Si–O(nbr), but that Si–O(br) will be longer than Si–O(nbr) when O(br)–Si–O(nbr) are narrower than O(nbr)–Si–O(nbr) and Si–O(br) and Si–O(nbr) will nearly equal when all O–Si–O angles are close to 109.47°, even though the Si–O–Si linkage is linear (Louisnathan and Gibbs, 1972a).

## The Double Bond Character in the Si–O Bond

Theoretical investigations based on EHMO calculations (Louisnathan and Gibbs, 1972b) indicate that only in the case of ideal $T_d$ $SiO_4$ tetrahedron the $3d(e)$–$2p$ $\pi$–bonds contribute significantly to the $n$(Si–O). When O–Si–O angular distortions are present, the $d$–$p$ $\pi$–bonding is established by the use of such $3d$ orbitals that are consistent with the point-group of the silicate ion and the $3p$–$2p$ $\pi$–bonds also begin to contribute significantly to the $n$(Si–O). In fact, the relationship between Si–O–Si angle and Si–O(br) bonds can be explained on the basis of the $3p$–$2p$ $\pi$–bond order as well as by the $3d$–$2p$ $\pi$–bond order. Despite that our calculations are not designed

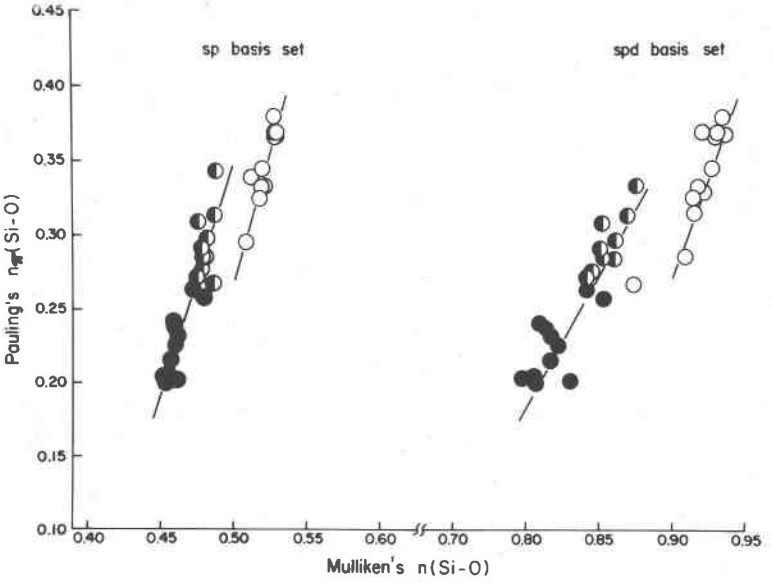


FIG. 11. Pauling's $n_\pi$(Si–O) vs. Mulliken's $n$(Si–O) for the eleven olivines calculated with Si(*spd*) basis set.

to test whether or not silicon 'uses' its 3*d* orbitals, the calculations clearly suggest that $\pi$–bonding plays an important role in determining the variations in Si–O distance. When an Si–O bond is involved with widest O–Si–O angles both $\sigma$– and $\pi$–bond populations increase, or when the tetrahedral angles associated with bond are the narrowest both $\sigma$– and $\pi$–bond populations decrease. Thus empirical correlations, like the relationship between Si–O(br) bond length and Si–O–Si angle, become amenable for interpretation by using the $\pi$–bonding theory (*d–p* or *p–p*) alone without having to closely examine the bond order pertubations in the $\sigma$–framework. Pauling (1952) rationalized a semi–empirical relationship between bond length and the $\pi$–bond character, $n_\pi$(Si–O). When the $n_\pi$(Si–O) calculated using the observed bond lengths are plotted as a function of $n$(Si–O), strong correlations emerge (Fig. 11), suggesting that arguments based on $\pi$–bonding model are not contradictory to arguments based on $\sigma$– plus $\pi$–bonding schemes. In this respect the Si–O $\pi$–bonds behave very much like C–C, C–N, C–O, etc. $\pi$–bonds in hydrocarbons and other conjugated systems, where the simple $\pi$–electron Hückel theory has found a large measure of success in explaining bond lengths, chemical reactivities and many other properties.

ACKNOWLEDGMENTS

We wish to thank our colleague and friend Professor F. D. Bloss who offered a number of helpful criticisms when part of this paper was presented at the 1971 annual GSA–MSA meeting. It is also a pleasure to thank D. W. J. Cruickshank, Visiting Professor of Geochemistry at V.P.I. & S.U., for constructive criticisms of the manuscript as well as for stimulating discussion of his *ab initio* calculations for orthosilicic acid and the stereochemistry of silicates in general. This study was supported by NSF grants GA-12702, GA-30864X, and GU-1392 and the Research Associateship for S. J. Louisnathan was supported by NSF Departmental Development Grant GU-3192.

REFERENCES

BASCHE, H., A. VISTE, AND H. B. GRAY (1965) Valence orbital ionization potentials from atomic spectral data. *Theoret. Chim. Acta,* **3**, 458–464.

BAUR, W. H. (1970) Bond length variation and distorted coordination polyhedra in inorganic crystals. *Trans. Amer. Crystallogr. Ass.* **6**, 125–155.

——— (1971) The prediction of bond length variations in silicon–oxygen bonds. *Amer. Mineral.* **56**, 1573–1599.

BIRLE, J. D., G. V. GIBBS, P. D. MOORE, AND J. B. SMITH (1968) Crystal structure of natural olivines. *Amer. Mineral.* **53**, 807–823.

BROWN, G. E., AND G. V. GIBBS (1970) Stereochemistry and ordering in the tetrahedral portion of silicates. *Amer. Mineral.* **55**, 1589–1607.

CLEMENTI, E., AND D. L. RAIMONDI (1963) Atomic screening constant from SCF functions. *J. Chem. Soc.* **38**, 2686–2689.

COLLINS, G. A. D., D. W. J. CRUICKSHANK, AND A. BREEZE (1972) *Ab initio* calculations on the silicate ion, orthosilicic acid and their $L_{2,3}$ X-ray spectra. *J. Chem. Soc., Faraday Trans. II,* **68**, 1189–1195.

GIBBS, G. V., M. M. HAMIL, S. J. LOUISNATHAN, L. S. BARTELL, AND H. YOW (1972) Correlations between Si–O bond length, Si–O–Si angle and bond overlap populations calculated using extended Hückel molecular orbital theory. *Amer. Mineral.* **57**, 1578–1613.

GRAY, H. B. (1964) *Electrons and Chemical Bonding.* Benjamin, New York.

LOUISNATHAN, S. J. (1969a) Refinement of the crystal structure of hardystonite. *Z. Kristallogr.* **130**, 427–437.

——— (1969b) The nature of Mg–Al–Si ordering in melilites, $(Ca,Na)_2$ — $(Mg,Al)$ $(Al,Si)_2O_7$ and the crystal structure of resnoite, $Ba_2(TiO)Si_2O_7$. Ph.D. Thesis, University of Chicago.

——— (1970) The crystal structure of synthetic soda melilite, $CaNaAlSi_2O_7$. *Z. Kristallogr.* **131**, 314–321.

———, AND G. V. GIBBS (1972a) Aluminum–silicon distribution in zunyite. *Amer. Mineral.* **57**, 1089–1108.

———, AND ——— (1972b) The effect of tetrahedral angles on the Si–O bond overlap populations in isolated tetrahedra. *Amer. Mineral.* **57**, 1614–1642.

MCDONALD, W. S., AND D. W. J. CRUICKSHANK (1967) A reinvestigation of the structure of sodium metasilicate, $Na_2SiO_3$. *Acta Crystallogr.* **22**, 37–43.

MULLIKEN, R. S. (1955) I. Electronic population analysis on LCAO-MO molecular wave functions. *J. Chem. Phys.* **23**, 1833–1840. II. Overlap populations, bond orders, and covalent bond energies. *J. Chem. Phys.* **23**, 1841–1846.

PAULING, LINUS (1929) The principles determining the structure of complex ionic crystals. *J. Amer. Chem. Soc.* **51**, 1010–1026.

——— (1952) Interatomic distances and bond character in the oxygen acids and related substances. *J. Phys. Chem.* **56**, 361–365.

——— (1960) *The Nature of the Chemical Bond, 3rd ed.* Cornell Univ. Press, Ithaca, New York.

RIBBE, P. H., AND G. V. GIBBS (1971) Crystal structures of the humite minerals: III. Mg/Fe ordering in humite and its relation to other ferromagnesian silicates. *Amer. Mineral.* **56**, 1155–1173.

SMITH, J. V. (1953) Reexamination of the crystal structure of melilite. *Amer. Mineral.* **38**, 643–661.

*Manuscript received, December 22, 1971; accepted for publication, June 13, 1972.*